Available online at www.sciencedirect.com
ScienceDirect
Polymer Degradation and Stability 93 (2008) 731–738
Polymer Degradation and Stability
www.elsevier.com/locate/polydegstab

Degradation patterns and surface wettability of electrospun fibrous mats

Wenguo Cui, Xiaohong Li*, Shaobing Zhou, Jie Weng

Key Laboratory of Advanced Technologies of Materials, Ministry of Education, School of Materials Science and Engineering, Southwest Jiaotong University, Chengdu 610031, PR China

Received 23 October 2007; received in revised form 7 December 2007; accepted 8 December 2007
Available online 20 February 2008

Abstract

Degradation profiles and surface wettability are critical for optimal application of electrospun fibrous mats as drug carriers, tissue growth scaffolds and wound dressing materials. The effect of surface morphologies and chemical groups on surface wettability, and the resulting matrix degradation profiles were firstly assessed for electrospun poly(D,L-lactide) (PDLLA) and poly(D,L-lactide)-poly(ethylene glycol) (PELA) fibers. The air entrapment between the fiber interfaces clarified the effects of various surface morphologies on the surface wettability. Chemical groups with lower binding energy were enriched on the fiber surface due to the high voltage of the electrospinning process, and a surface erosion pattern was detected in the degradation of electrospun PDLLA fibers, which was quite different from the bulk degradation pattern for other forms of PDLLA. Contributed by the hydrophilic poly(ethylene glycol) segments, the degradation of electrospun PELA fibers with hydrophobic surface followed a pattern different from surface erosion and typical bulk degradation.

Keywords: Degradation pattern; Surface wettability; Electrospinning; Surface morphology; Surface erosion

1. Introduction

Polymer nanofibers have attracted increasing attentions in the last 10 years. The very large surface area to volume ratio, flexibility in surface functionalities, superior mechanical performance, and versatility of design are some of the characteristics that make polymer nanofibers optimal candidates for many important applications such as protective clothing, catalysis, electronics, biomedicine, and filtration [1]. Several fabrication techniques such as electrospinning [2], melt-blown [3], phase separation [4], self-assembly [5], and template synthesis [6] have been employed to produce suitable polymer nanofibers for different purposes. Amongst these, electrospinning is the most popular and preferred technique to use. Electrospinning is a versatile polymer processing technique, in which a stream of polymer solution or melt is subjected to a high electric field resulting in the formation of nano-dimensional fibers. Surface wettability plays important roles in the degradation pattern of electrospun nanofibers, which is crucial for their end uses as scaffolds for tissue engineering, tissue repair substitutes, wound dressing materials and carriers for drug delivery [7].

Flexibility of the electrospinning process allows co-spinning polymers with drugs or proteins thereby making non-woven nanofibrous mats as drug delivery matrices. It is indicated that the primary factor affecting drug release profiles is matrix degradation. Kim et al. investigated the amphiphilic block copolymer poly(D,L-lactide)-poly(ethylene glycol) (PELA) electrospun fibers. Compared to the electrospun poly(lactide-*co*-glycolide) (PLGA)-based nanofibrous mats, the cumulative amount of the released drug was reduced at earlier time points and the drug release rate was prolonged at longer times [8]. Studies have shown that cells seeded on biodegradable polymeric nanofiber mats can attach, proliferate and maintain their phenotype expression [9]. Electrospun nanofibers have been used as scaffolds for engineering tissues such as cartilages [10], bones [11], arterial blood vessels [12], heart [13], and nerves [14]. But the surface wettability and degradation profiles of scaffolds are critical for favorable cellular responses, which should support attachment, proliferation and differentiation of cells, as well as maintaining suitable mechanical properties

* Corresponding author. Tel.: +86 28 87634023; fax: +86 28 87634649.
E-mail address: xhli@swjtu.edu.cn (X. Li).

0141-3910/$ - see front matter © 2007 Elsevier Ltd. All rights reserved.
doi:10.1016/j.polymdegradstab.2007.12.002

until tissues are regenerated at the injured site. Ideally, the degradation rates of the scaffold should be matched with the rate of neo-tissue formation so as to provide a smooth transition of the load transfer from the scaffold to the tissue. Boland et al. indicated that the surface hydrolysis of ester bonds by hydrochloric acid, which exposes carboxylic acid and alcohol groups, improved the ability of cells to adhere to the surface [15]. Chua et al. found that surface-aminated electrospun nanofibers enhanced the adhesion and expansion of human umbilical cord blood hematopoietic progenitor cells [16]. Polymeric nanofibers were also used as temporary wound dressing and haemostatic devices due to the controllable porous structure, which showed controlled evaporative water loss as well as excellent oxygen permeability, promoted fluid drainage ability, but inhibited exogenous microorganism invasion [17]. Zong et al. investigated electrospun non-woven bioabsorbable nanofibrous membranes of PLGA, which were effective to reduce adhesions at the site of injury using a rat model [18]. The unique morphology of electrospun membranes and the relatively hydrophobic property provided a comfortable texture and easy handling ability for the electrospun membranes during surgery.

The already published work clearly shows that chemical composition and surface structure determine the hydrophobic behaviors of electrospun fibers. Zhu et al. described a method to form hydrophobic surfaces using poly(hydroxybutyrate-*co*-hydroxyvalerate), a kind of intrinsically hydrophilic material, and found that beads on these surfaces caused water contact angles (WCAs) ranging from 110.7° to 158.1° [19]. Block copolymer poly(styrene-*b*-dimethylsiloxane) was electrospun by Ma et al., and the non-woven fibrous mats were superhydrophobic with a contact angle of 163°. The superhydrophobicity was attributed to the combined effects of surface enrichment of siloxane as revealed by X-ray photoelectron spectroscopy (XPS) and surface roughness of the electrospun mat itself [20]. Deitzel et al. found that the atomic percentage of fluorine in the near surface region of the electrospun fibers was about double the atomic percentage of fluorine found in a bulk sample of the random copolymer of methyl methacrylate and tetrahydroperfluorooctyl acrylate [21]. But most of the published works used non-degradable polymer as a model and one or two aspects of these factors, such as fiber characteristics, surface groups and surface morphologies, have been investigated individually on the hydrophobic properties. Degradable polymers, such as poly(D,L-lactide) (PDLLA), PLGA and PELA have been investigated because of their biocompatibility and the flexibility they offer in terms of degradation profiles [22], which enable researchers to tailor these polymers to specific biomedical applications and have shown potentials as drug carriers and tissue growth scaffolds [23]. To the best of our knowledge, a systematic study on the wettability and degradation patterns of electrospun fibrous mats of PDLLA and PELA with various morphologies has not been reported before.

This study was designed to investigate the effect of surface morphology and chemical groups on surface wettability, and the resulting matrix degradation profiles of electrospun PDLLA and PELA fibers. Various surface morphologies, such as different fiber diameters and pore sizes of the fibrous matrix, and different surface roughness of individual fibers, were created on electrospun fibrous mats. During previous orthogonal table design experiment, quantitative relations between fiber properties and electrospinning parameters have been established for electrospun PDLLA fibers [24]. The optimized parameters were applied in the current study to prepare fibrous mats with predetermined sizes and morphologies.

2. Experimental section

2.1. Materials

PDLLA ($M_w = 53$ kDa, $M_w/M_n = 1.35$, D/L = 50/50) and PELA ($M_w = 51$ kDa, $M_w/M_n = 1.26$) with 10% of poly(ethylene glycol) (PEG) content were prepared by bulk ring-opening polymerization of lactide or lactide/PEG using stannous chloride as initiator [25]. The actual PEG content of PELA was calculated from the integral height of hydrogen shown by ^{1}H NMR (Varian FT-80A, Harbor City, CA). The molecular weights of PELA and PDLLA were determined by gel permeation chromatography (GPC, waters 2695 and 2414, Milford, MA) with Styragel HT 4 column using polystyrene as standard. The mobile phase was tetrahydrofuran (THF) using a regularity elution at a flow rate of 1.0 ml/min. All other chemicals and solvents were of reagent grade or better.

2.2. Preparation of electrospun fibrous mats

The electrospinning process was performed as described elsewhere [24]. Briefly, the electrospinning apparatus was equipped with a high-voltage statitron (Tianjing High Voltage Power Supply Co., Tianjing, China) of maximal voltage of 50 kV. The polymer solution was added in a 2 ml syringe attached to a circular-shaped metal syringe needle as nozzle. An oblong counter electrode was located about 15 cm from the capillary tip. The flow rate of the polymer solution was controlled by a precision pump (Zhejiang University Medical Instrument Co., Hangzhou, China) to maintain a steady flow from the capillary outlet. All the non-woven fibrous mats were vacuum dried at room temperature for 2 d to completely remove any solvent residue. Through optimizing such process parameters as polymer concentration, applied voltage, flow velocity and nozzle size based on previous investigations [24], electrospun fibrous mats were prepared with different sizes of fibers and sizes of pores between fibers. To create rough surface on individual fibers, calcium nitrate was dissolved with PDLLA in THF solution. The resulting electrospun fibrous mats were incubated in ice water for 2 d to remove calcium nitrate from the fiber surface, and vacuum dried at room temperature for additional 2 d before further characterization.

2.3. Fiber characterization

The diameters of electrospun fibers and morphologies of fibrous mats were investigated by scanning electron microscope (SEM, FEI Quanta 200, the Netherlands) equipped with field-emission gun (20 kV) and Robinson detector after

2 min of gold coating to minimize charging effect. The fiber diameter was measured from SEM images with the magnification of 10,000, and five images were used for each fibrous sample. From each image, at least 20 different fibers and 200 different segments were randomly selected and their diameter measured to generate an average fiber diameter by using the tool of Photoshop 10.0 edition. The surface pore sizes (converted to a round shape) [26] of the fibrous mats were also evaluated from SEM images with the magnification of 2000 through the similar process as described above.

2.4. WCA measurement

Electrospun fibrous mats were collected on a flat aluminum foil. A drop of purified water was deposited onto the mat surface using a micro-syringe attached on the goniometer. The WCAs of water drops on the electrospun fibrous mat were measured on a Kruss GmbH DSA 100 Mk 2 goniometer (Hamburg, Germany) followed by image processing of sessile drop with DSA 1.8 software. At least 6 droplets were tested on different parts of each mat.

2.5. Surface analysis

Chemical compositions of the mat surface were determined by XPS (XSAM800, Kratos Ltd, Britain) using Mg Kα1,2 radiation, and data were processed by using Kratos VISION 2000. The overview spectra were taken between 50 and 1300 eV with an energy step of 0.5 eV using pass energy of 300 eV, while the detailed spectra of peaks of interest (Ols and Cls) were recorded with an energy step of 0.05 eV. In all cases, oxygen (O1s, 533.00 eV) and carbon (C1s, 285.00 eV) were detected at the surface in the survey spectra. Detailed analysis of the C1s regions was recorded over the binding energy range of 280.00–300.00 eV with pass energy of 150.00 eV. Charge referencing was performed using the C–H peak (285.00 eV) for PDLLA and PELA samples. The total acquisition time was 15 min for each sample. The overlapping peaks were resolved by the peak synthesis method, applying Gaussian peak components after Shirley type background subtraction.

2.6. In vitro degradation behaviors

The degradation behavior was evaluated from the morphological change, molecular weight reduction and mass loss. Pre-weighted pieces of electrospun non-woven fabrics and solvent casting films with initial thickness of about 150 μm each and initial weight of about 80 mg were incubated at 37 °C in 20.0 ml of pH 7.4, 154 mM phosphate buffered saline (PBS) containing 0.02% sodium azide as a bacteriostatic agent. At predetermined intervals, triplicate samples for each kind of fabrics or films were recovered, rinsed with distilled water to remove residual buffer salts, and dried to constant weight in a vacuum desiccator. The morphological change was estimated from SEM observation as mentioned above. The mass loss was determined gravimetrically by comparing the dry weight remaining at a specific time with the initial weight. The recovered and dried fabrics or films were dissolved in THF and filtered to eliminate insoluble residues. The molecular weight of recovered matrix polymer was determined using GPC as described above.

3. Results

3.1. Effect of surface morphology on the wettability of electrospun mats

Electrospun mats of different fiber diameters were obtained to test the effect on the surface wettability. Fig. 1a–c shows fibers were bead-free with different fiber sizes, and the electrospun mats had an average pore size of around 3.5 μm. The WCAs were $143.0 \pm 1.7°$, $127.3 \pm 2.7°$ and $102.7 \pm 2.1°$ for electrospun mats with fiber diameters of 0.6 ± 0.06 μm, 1.8 ± 0.2 μm and 2.4 ± 0.3 μm, respectively. The increase in the fiber diameters caused a significant decrease in WCA, which indicated that the topography of fibers with different diameters could influence the liquid–solid interface. More fibers were sprayed to the collector in the same time, and dense fibrous mats could be formed. Different pore sizes were obtained through adjusting processing parameters to study the effect on the surface wettability of fibrous mats. As shown in Fig. 1d–f, fibrous mats were obtained with different pore sizes, and the fibers were bead-free with an average diameter of around 0.7 μm. The WCAs were $134.0 \pm 2.4°$, $120.5 \pm 1.8°$ and $107.2 \pm 2.5°$ for fibrous mats with pores sizes of 2.1 ± 0.8 μm, 4.6 ± 1.1 μm and 6.2 ± 1.3 μm, respectively.

The surface morphologies of fibrous mat can be influenced by the larger topography of the ''web'' of electrospun fibers, as indicated above, and the surface topography of the fibers themselves. Calcium nitrate was co-spun into the PDLLA fibers, then, was removed to create rough surface on the fibers to investigate the effect of surface roughness on the wettability of fibrous mats. As shown in Fig. 2, pores of average diameter of about 100 nm were created on the fiber surface, and higher amount of calcium nitrate included in the electrospinning solution resulted in more pores formed on the fiber surface. The WCAs of fibers with porous surface were $141.7 \pm 2.2°$ and $147.5 \pm 1.7°$ for fibers prepared form electrospinning solution containing 10% (Fig. 2b) and 16.7% (Fig. 2c) of calcium nitrate, respectively, which were slightly larger than $133.2 \pm 1.9°$ for fibers with smooth surface (Fig. 2a).

3.2. Effect of electrospinning on chemical group remolding and surface wettability of electrospun fibrous mats

Electrospun fibrous mats of homopolymer PDLLA and copolymer PELA were determined with regard to the surface wettability and chemical group remolding, while solvent casting films were used as control. The WCAs of electrospun mat and casting film of PDLLA were $132.2 \pm 1.5°$ and $76.4 \pm 1.3°$, and those of PELA were $114.0 \pm 1.3°$ and $70.1 \pm 2.3°$, respectively. The chemical groups on the surface of casting films and electrospun mats of both PDLLA and

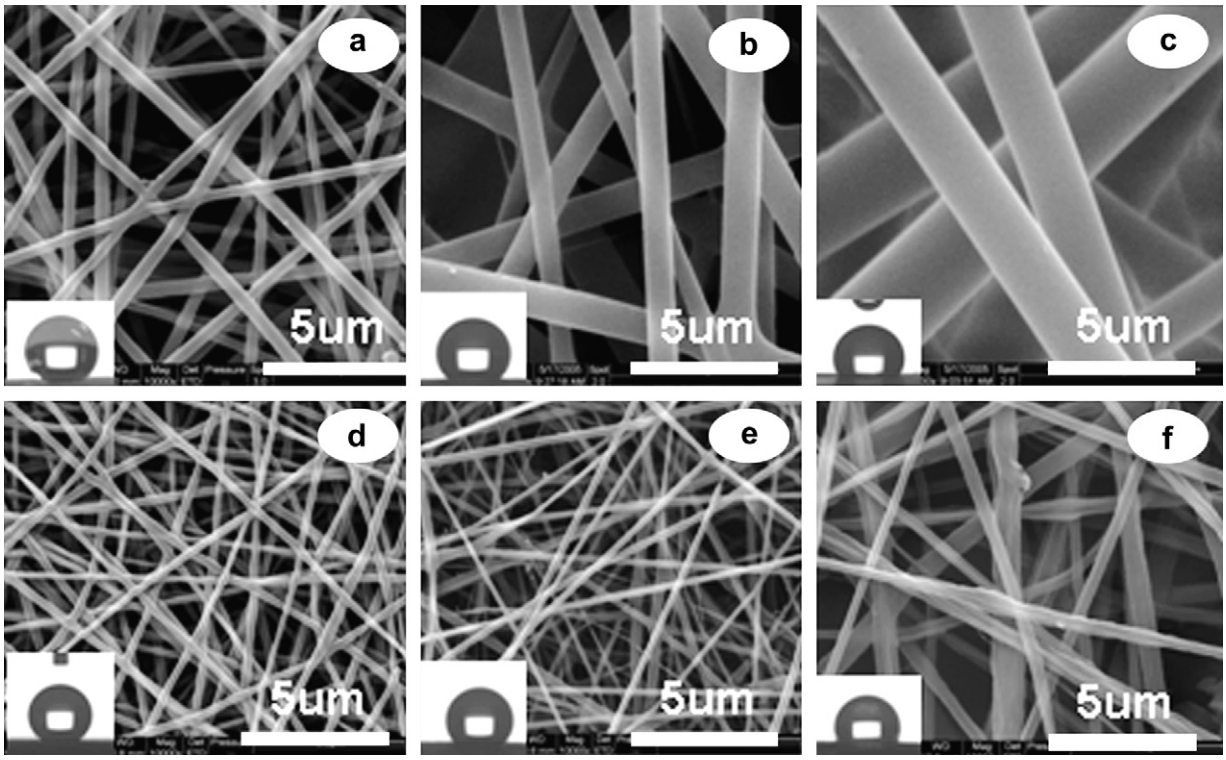

Fig. 1. SEM morphologies and WCA images of electrospun fibrous mats with average fiber sizes of 0.6 μm (a), 1.8 μm (b), and 2.4 μm (c), and with average pore sizes of 2.1 μm (d), 4.6 μm (e), and 6.2 μm (f).

PELA were determined by XPS to clarify the effect on the surface wettability. The C1s spectra of electrospun PDLLA and PELA fibrous mats are shown in Fig. 3, along with their chemical structures. In the C1s region of PDLLA casting film, three peaks of equal areas were observed corresponding to the methyl group (285.00 eV), the methine group (287.05 eV), and the ester group (289.20 eV). Four peaks were present in the C1s region of PELA casting film. Besides peaks from PDLLA, one peak centered at approximately 286.30 eV, resulted from the PEG block. Table 1 summarizes the peak assignments, the theoretical and experimental contents of each carbon environment. The numbers assigned to each peak will be used to identify the presence of these carbon environments in the data analysis for electrospun fibers.

As shown in Table 1, the experimental values of each peak of PDLLA and PELA casting films were very close to the theoretical ones based on all the carbon environments being present in their stoichiometric ratios. Fig. 3a showed the C1s region of PDLLA electrospun fibers, from which, without curve fitting, it was possible to make a number of qualitative statements about the differences in surface chemistry between the electrospun mats and casting films. The curve for PDLLA electrospun fibers displayed a significantly higher intensity in the methyl group region from 285.00 to 286.50 eV compared to the casting film. But lower intensities were observed in the methine and ester group region from 286.70 to 290.00 eV. It indicated that remodeling of chemical groups occurred after the electrospinning process, and significantly higher intensities

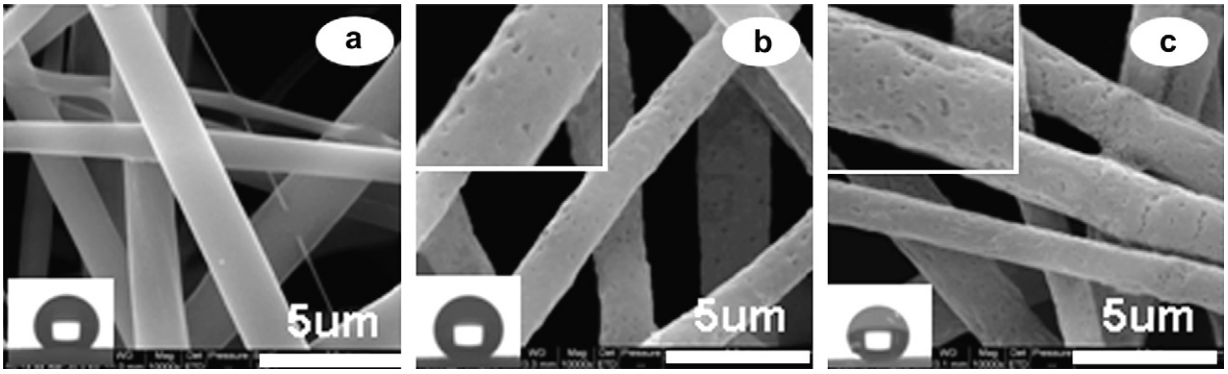

Fig. 2. SEM morphologies and WCA images of electrospun fibrous mats with smooth surface (a), and rough surface prepared from electrospinning solutions containing 10% (b) and 16.7% (c) of calcium nitrate (insertions showing higher magnifications).

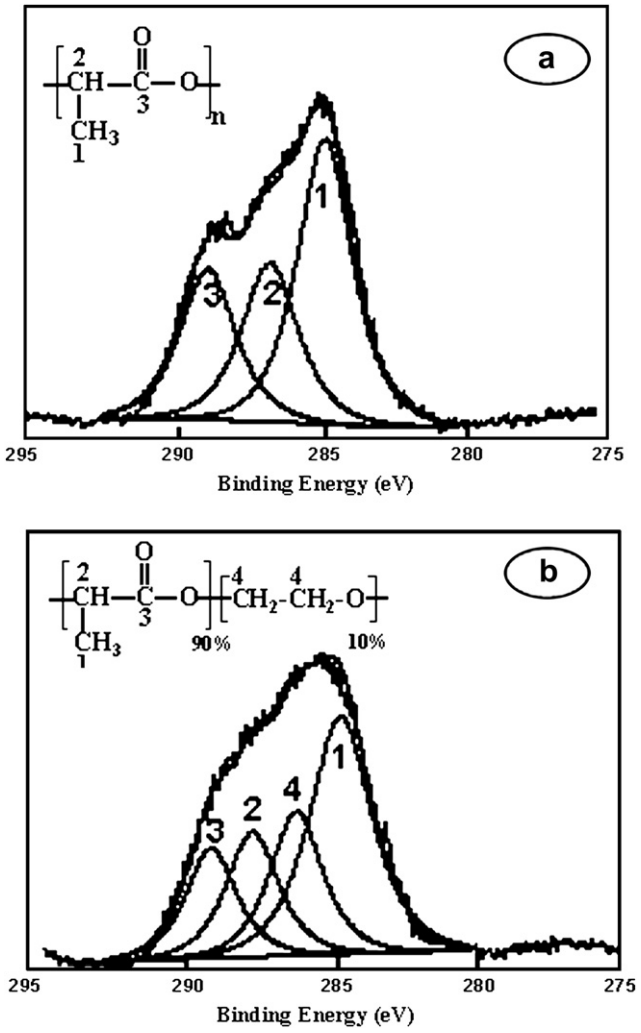

Fig. 3. C1s regions and the peak assignments of XPS signals for electrospun fibrous mats of PDLLA (a) and PELA (b).

of the lower binding energy groups displayed on electrospun fibers. As shown in Table 1, there was about 13% of increase in the content of methyl groups on the fiber surface. Fig. 3b shows that the changes of C1s spectra of PELA electrospun fibers were similar to those of PDLLA fibers. The significant deviation occurred at the binding energy of 285.00 and 286.30 eV, indicating the enrichment of lower binding energy of methyl groups on the surface and the increase in the contribution of PEG. As summarized in Table 1, there were about 9% and 16% of increase in the carbon environment of methyl group of PDLLA segment and methylene group of PEG segment, respectively.

3.3. In vitro degradation of electrospun fibrous mat

After being incubated into degradation medium, the non-woven fibrous mat floated, then suspended and immersed into the medium. Non-woven mat changed from shrinking to puffing bigger than previously described, meanwhile, fiber size increased and fiber space shrunk for all samples. Fig. 4 showed the morphology changes of PDLLA and PELA fibers after

Table 1
The experimental and theoretical contents of C1s regions of XPS signals for electrospun fibrous mats and solvent casting films of PDLLA and PELA

Peak	Binding energy (eV)	PDLLA			PELA		
		Fiber exp. (%)	Film exp. (%)	Theo. (%)	Fiber exp. (%)	Film exp. (%)	Theo. (%)
1	285.00	47.4	34.1	33.3	42.7	33.7	31.0
2	287.05	27.2	33.4	33.3	19.0	29.9	31.0
3	289.20	25.4	32.5	33.3	16.2	29.9	31.0
4	286.30	N.A.	N.A.	N.A.	22.1	6.5	7.0

incubation for 4 and 10 weeks. At week 4 all fibers were swollen compared with the original formation (Fig. 4a,d), due to the chain relaxation of matrix polymer after being incubated into the medium with elevated temperature. And the shrinkage, curliness and congeries of fibers could be easily found for PDLLA and PELA fibers at week 4 (Fig. 4b,e). Significant conglutination was observed at week 10 for all samples (Fig. 4c,f) due to the degradation of matrix polymer, and the fiber size decreased due to mass loss. There were stronger rupture and conglutination of PELA fibers (Fig. 4f) compared to PDLLA fibers (Fig. 4c).

The degradation of electrospun fibers and solvent casting films of PDLLA and PELA was determined with regard to mass loss of the fiber matrix and molecular weight reduction of the matrix polymer. Gravimetric evaluation of mass loss during incubation is summarized in Fig. 5a. The mass loss of the fibers and films in the early stage may result from the dissolution of oligomers into the medium. At week 8 there was 10% of mass loss for casting films of PDLLA and PELA, while 20% of mass loss was observed for electrospun fibrous mats. The mass loss became more significant for casting films in the later stage, and the differences were narrowed between the mass loss of fibrous mats and casting films. At week 10 there were 23.5% and 27.0% of mass losses for casting films of PDLLA and PELA, while 24.7% and 28.2% were detected for fibrous mats of PDLLA and PELA, respectively. Fig. 5b showed the molecular weight reduction of polymer matrix of fibrous mats and polymer films. Less than 10% of molecular weight reduction was found for electrospun fibrous mat of PDLLA, but the molecular weight decreased gradually with incubation time and around 66.0% of molecular weight loss was detected after 10 weeks of incubation for casting films. There were a total of 51.0% and 69.0% of molecular weight loss for fibrous mat and casting film of PELA after 10 weeks of incubation, respectively. Different degradation patterns should exist between the electrospun fibers and solvent casting films, resulting from their different surface wettability.

4. Discussion

Degradation profiles and surface wettability are critical for optimal application of electrospun fibrous mat as drug carriers, tissue growth scaffolds and wound dressing materials. It has been noted that the secret of water repellency of lotus leaves is due to surface roughness caused by branchlike nanostructures on top of the micropapillae and the low surface energy epicuticular wax [27]. During the electrospinning process, the high surface tension at the air/polymer interface, the aligning effect of

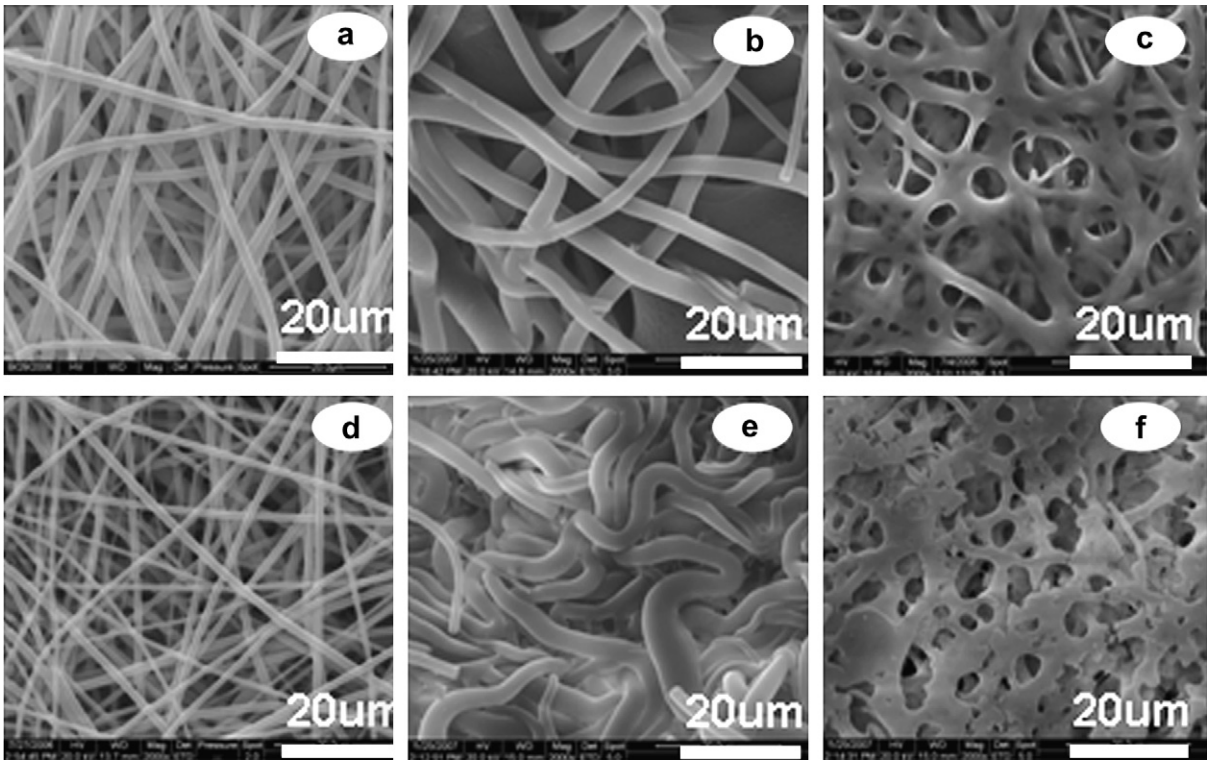

Fig. 4. SEM morphologies of electrospun fibers of PDLLA (a, b, c) and PELA (d, e, f) before incubation (a, d), after incubation for 4 (b, e) and 10 weeks (c, f) at 37 °C in pH 7.4, 154 mM PBS.

the elongational flow and the rapid solidification are believed to have some effects on the surface morphologies. Generally, the WCA value of the solvent casting PDLLA film was only 76.4°, and more hydrophobic surface was observed for electrospun fibrous mats (Fig. 1). Various surface morphologies of electrospun fibrous mat showed different surface roughness, which may result in different volumes of air to be trapped between interfaces of fibers and water. Construing the system of fiber structure, the surface roughness degree of electrospun mats increased with the decrease in fiber diameters and the pore sizes between fibers, leading to higher air entrapment in the surface pores. So, larger WCAs were obtained for electrospun mats with smaller fiber diameter (Fig. 1a–c) and pore sizes (Fig. 1d–f). The relatively higher WCA for fibrous mats with rough surface of individual fibers, created by removal of calcium nitrate being electrospun into the fiber matrix (Fig. 2), may be caused by the holes which could trap more air in the inter-space than fibers with smooth surface. So the surface roughness of the fibrous mats resulted in air entrapment between fiber interfaces to show effects on WCA values.

During the electrospinning process, the high voltage, high-speed swing and solvent evaporation may have effect on reconstructing group distribution. Ma et al. showed the surface enrichment of siloxane after electrospinning block copolymer poly(styrene-*b*-dimethylsiloxane) [20]. Deitzel et al. indicated that surface fluorine groups of the electrospun fiber were about double that found in a bulk sample of the random copolymer [21]. In this study, surface groups of electrospun fibrous mats and solvent casting films were analyzed by XPS. It indicated that groups of lower binding energy could be enriched on the fiber surface through the electrospinning process. The methyl groups of PDLLA with binding energy of 285.00 eV were hydrophobic, and got enriched on the surface of electrospun fibers (Fig. 3a and Table 1). For the electrospun PELA fibrous mat, methyl groups of PDLLA segment with binding energy of 285.00 eV and methylene groups of PEG segment with that of 286.30 eV were enriched (Fig. 3b and Table 1). Fig. 6 showed the schematic illustration of the remolding of chemical groups on the surface of electrospun fibers of PDLLA and PELA.

Surface chemical groups were indicated to be one reason causing the surface wettability of the electrospun fibrous mats. Poly(ethylene terephthalate) electrospun fiber mats showed very high water contact angle. But after surface modification either by poly(methacrylic acid) grafting or by gelatin grafting, the water drop was suddenly sucked into the electrospun fibrous mat, giving a zero water contact angle [28]. Chua et al. found the contact angle of the electrospun polyethersulfone fiber mesh decreased from 133° to 0° after poly(methacrylic acid) grafting [16]. In the current system, the hydrophobic surface character of electrospun fibrous mats should be attributed to the enrichment of methyl groups. So the conclusion could be got that the surface topology and surface chemical groups of electrospun fibers could be of influence on the values of water contact angles.

The degradation behavior of matrix polymer is one of the most important aspects for the end application as drug carriers and tissue growth scaffolds. The processes involved in the erosion of a degradable polymer are complicated. Water enters the polymer bulk, which might be accompanied by swelling. The intrusion of water triggers the chemical polymer

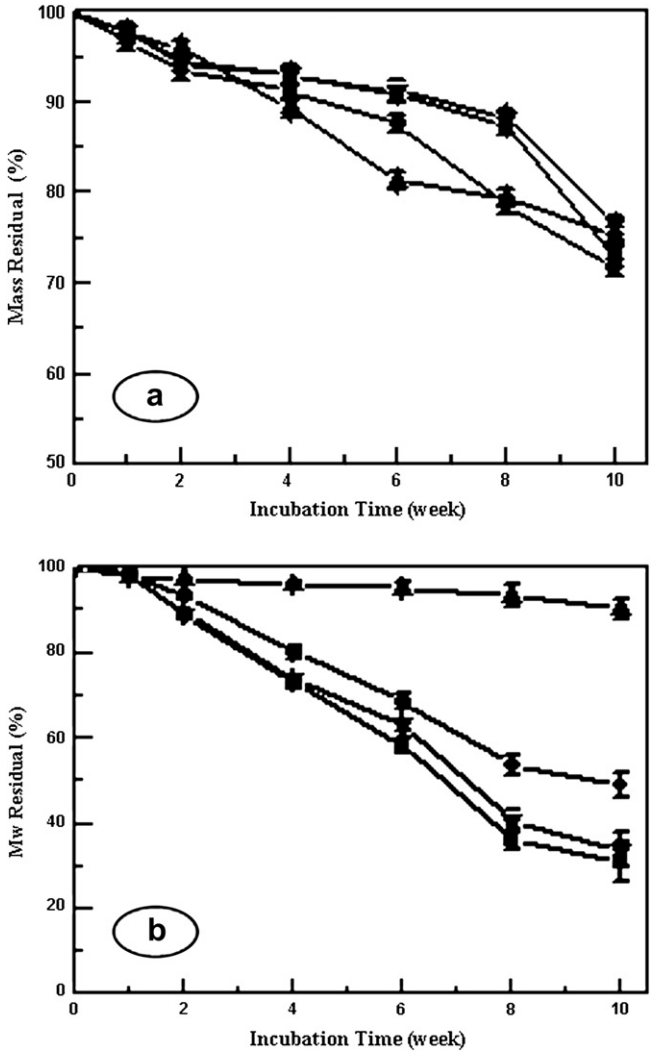

Fig. 5. Mass residual (a) and molecular weight residual (b) of electrospun fibrous mats of PDLLA (up triangle) and PELA (diamond), and of solvent casting films of PDLLA (down triangle) and PELA (square) after incubation at 37 °C in pH 7.4, 154 mM PBS.

degradation, leading to the creation of oligomers and monomers. Progressive degradation changes the microstructure of the bulk through the formation of pores, via which oligomers and monomers are released. So the type of chemical bond, compositions and water uptake are the most important factors that influence the velocity of polymer degradation reaction. The degradation of PDLLA and PLGA could be optimized by physically and chemically modifying the surface wettability of polymer matrix. Davies et al. found that the degradation behavior was determined by the chemical composition and the molecular organization of the material surface, which also had influence on the surface wettability [29].

As shown in Fig. 5, electrospun fibrous mats and casting films of PDLLA and PELA had different degradation profiles. The molecular weight residuals for PDLLA and PELA casting films were about 40.7% and 36.3% at week 8, respectively, and the mass losses were about 11.6% and 12.5%, respectively. The molecular weight reduction was much higher than mass loss, which showed a typical bulk degradation pattern. For

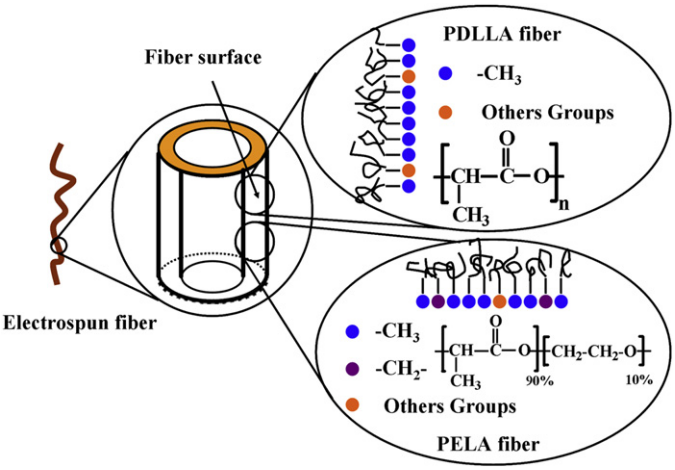

Fig. 6. Schematic illustration of the distribution of chemical groups on the surface of electrospun PDLLA and PELA fibers.

electrospun PDLLA fibrous mats, however, 20.6% of mass loss was detected at week 8, while only 6.5% of molecular weight reduction, which showed a surface erosion pattern. The surface erosion pattern of electrospun fibers was quite different from the bulk degradation, which was usually detected for other forms of PDLLA. The difference between the breakdown velocity of chemical bond of matrix polymer and the distribution speed of water into the polymer matrix would determine the degradation mechanism for most of the degradable polymers. Degradation based on surface erosion mechanism would occur when the water penetration was slower than the matrix breakdown. The different degradation patterns between electrospun fibrous mat and casting film of PDLLA mostly resulted from the different water diffusion rates from the medium into fiber matrices. During the electrospinning process, chemical groups of lower binding energy were found to be enriched on the fiber surface, which enhanced the hydrophobicity of the fibrous mat. As mentioned above, the WCA of electrospun fibrous mat of PDLLA was $132.2 \pm 1.5°$, which was significantly higher than those of PELA fibrous mats ($114.0 \pm 1.3°$) and PDLLA casting films ($70.1 \pm 2.3°$). The hydrophobic surface resulted in slower water distribution from the medium to the fiber matrix. As shown in Fig. 5, the mass loss and molecular weight reduction for electrospun PELA fibers were 21.3% and 46.3% at week 8, respectively, which showed a degradation pattern between surface erosion and typical bulk degradation. The molecular weight reduction and mass loss of electrospun PELA fiber were much higher than those of PDLLA fibers. For PELA fibrous mat, larger amount of methyl groups of PDLLA segment could also delay the hydrolytic reaction. And different degradation patterns between electrospun fibrous mats of PELA and PDLLA were due to hydrophilic group contributed by PEG segments enriched on the fiber surface (Fig. 3b and Table 1).

Electrospun PDLLA fibrous mat with different fiber diameters and surface pore sizes resulted in hydrophobic surfaces with different WCA values (Fig. 1), but there was no significant difference in the degradation profiles (data not shown). When incubated into buffer solution, fibrous mats happened to shrink and single fiber happened to swell in the later

period of incubation (Fig. 4). The surface morphologies of electrospun fibrous mats could be restructured, and similar surface morphologies were shaped after shrinking and swelling. In conclusion, significant differences were determined in terms of degradation patterns of electrospun fibrous mats and solvent casting films of PDLLA and PELA. The high water repellent property of electrospun PDLLA fibers led to slower water penetration into the fibrous mats, which may be attributed to the degradation profiles of surface erosion. Therefore, the conclusion could be got that the enrichment of chemical element or groups due to high voltage of electrospinning process should play great roles in the degradation patterns of electrospun fibrous mats.

5. Conclusions

Fibrous mats with different sizes of fibers and surface pores between fibers, and with rough surface of individual fibers were obtained. The effect of surface morphologies on the wettability was determined. The surface roughness of the fibrous mat resulted in air entrapment between fiber interfaces, and air entrapment showed effects on WCA values. The electrospinning process resulted in enrichment of chemical groups with lower binding energy on the fiber surface, which was found to determine the surface wettability. The methyl groups enriched on the fiber surface delayed the rate of water penetration, and surface erosion was detected in the degradation of electrospun PDLLA fibrous mat. These findings could achieve a better use of electrospun fibers in biomedical and related fields.

Acknowledgements

This work was supported by National Natural Science Foundation of China (30570501), Program for New Century Excellent Talents in University (NECT-06-0801), Specialized Research Fund for the Doctoral Program of Higher Education (20050613025), Fok Ying Tong Education Foundation (104032), Ministry of Education of China.

References

[1] Katarzyna M, Sawicka PG. Electrospun composite nanofibers for functional applications. J Nanopart Res 2006;8:769–71.
[2] Huang ZM, Zhang YZ, Kotaki M, Ramakrishna S. A review on polymer nanofibers by electrospinning and their applications in nanocomposites. Compos Sci Technol 2003;63:2224–53.
[3] Ondarcuhu T, Joachim C. Drawing a single nanofiber over hundreds of microns. Europhys Lett 1998;42:215–20.
[4] Ma PX, Zhang R. Synthetic nano-scale fibrous extracellular matrix. J Biomed Mater Res 1999;46:60–72.
[5] Whitesides GM, Grzybowski BJ. Self-assembly at all scales. Science 2002;295:2418–21.
[6] Martin CR. Membrane-based synthesis of nanomaterials. Chem Mater 1996;8:1739–46.
[7] Cui WG, Li XH, Zhu XL, Yu G, Zhou SB, Weng J. Investigation of drug release and matrix degradation of electrospun poly(DL-lactide) fibers with paracetanol inoculation. Biomacromolecules 2006;7:1623–9.
[8] Kim K, Luu YK, Chang C, Fang D, Hsiao BS, Chu B, et al. Incorporation and controlled release of a hydrophilic antibiotic using poly(lactide-*co*-glycolide)-based electrospun nanofibrous scaffolds. J Controlled Release 2004;98:47–56.
[9] Yoshimoto H, Shin YM, Terai H, Vacanti JP. A biodegradable nanofiber scaffold by electrospinning and its potential for bone tissue engineering. Biomaterials 2003;24:2077–82.
[10] Rho KS, Jeong L, Lee G, Seo BM, Park YJ, Hong SD, et al. Electrospinning of collagen nanofibers: effects on the behavior of normal human keratinocytes and early-stage wound healing. Biomaterials 2006;27:1452–61.
[11] Chen JL, Chu B, Hsiao BS. Mineralization of hydroxyapatite in electrospun nanofibrous poly(L-lactic acid) scaffolds. J Biomed Mater Res 2006;79A:307–17.
[12] Xu CY, Inai R, Kotaki M, Ramakrishna S. Aligned biodegradable nanofibrous structure: a potential scaffold for blood vessel engineering. Biomaterials 2004;25:877–86.
[13] Zong XH, Bien H, Chung CY, Yin LH, Fang DF, Hsiao BS, et al. Electrospun fine-textured scaffolds for heart tissue constructs. Biomaterials 2005;26:5330–8.
[14] Smith LA, Ma PX. Nano-fibrous scaffolds for tissue engineering. Colloid Surf B 2004;39:125–31.
[15] Boland ED, Telemeco TA, Simpson DG, Wnek GE, Bowlin GL. Utilizing acid pretreatment and electrospinning to improve biocompatibility of poly(glycolic acid) for tissue engineering. J Biomed Mater Res 2004;71B:144–52.
[16] Chua KN, Chai C, Lee PC, Tang YN, Ramakrishna S, Leong KW, et al. Surface-aminated electrospun nanofibers enhance adhesion and expansion of human umbilical cord blood hematopoietic stem/progenitor cells. Biomaterials 2006;27:6043–51.
[17] Khil MS, Cha DL, Kim HY, Kim IS, Bhattarai N. Electrospun nanofibrous polyurethane membrane as wound dressing. J Biomed Mater Res 2003;67B:675–9.
[18] Zong XH, Li S, Chen ME, Garlick B, Kim KS, Fang DF, et al. Prevention of postsurgery-induced abdominal adhesions by electrospun bioabsorbable nanofibrous poly(lactide-*co*-glycolide)-based membranes. Ann Surg 2004;240:910–5.
[19] Zhu MF, Zuo WW, Yu H, Yang W, Chen YM. Superhydrophobic surface directly created by electrospinning based on hydrophilic material. J Mater Sci 2006;41:3793–7.
[20] Ma ML, Hill RM, Lowery JL, Fridrikh SV, Rutledge GC. Electrospun poly(styrene-*block*-dimethylsiloxane) block copolymer fibers exhibiting superhydrophobicity. Langmuir 2005;21:5549–54.
[21] Deitzel JM, Kosik W, McKnight SH, Beck-Tan NC, DeSimone JM, Crette SJ. Electrospinning of polymer nanofibers with special surface chemistry. Polymer 2002;43:1025–9.
[22] Kissel T, Li YX, Volland C, Gorich S, Koneberg R. Parenteral protein delivery systems using biodegradable ABA-block copolymers. J Controlled Release 1996;39:315–21.
[23] Zhou SB, Liao XY, Li XH, Deng XM, Li HM. Poly-D,L-lactide-*co*-poly(ethylene glycol) microspheres as potential vaccine delivery systems. J Controlled Release 2003;86:195–205.
[24] Cui WG, Li XH, Zhou SB, Weng J. Investigation on process parameters of electrospinning system through orthogonal experimental design. J Appl Polym Sci 2007;103:3105–12.
[25] Deng XM, Xiong CD, Cheng LM. Synthesis and characterization of block copolymer from lactide and poly(ethylene glycol). J Polym Sci Part C 1990;28:411–6.
[26] Diamond S. Mercury porosimetry: an inappropriate method for the measurement of pore size distributions in cement-based materials. Cement Concrete Res 2000;30:1517–25.
[27] Cheng YT, Rodak DE, Wong CA, Hayden CA. Effects of micro- and nano-structures on the self-cleaning behaviour of lotus leaves. Nanotechnology 2006;17:1359–62.
[28] Ma ZW, Kotaki M, Yong T, He W, Ramakrishna S. Surface engineering of electrospun polyethylene terephthalate (PET) nanofibers towards development of a new material for blood vessel engineering. Biomaterials 2005;26:2527–36.
[29] Davies MC, Shakesheff KM, Shard AG, Domb A, Roberts CJ, Tendler SJB, et al. Surface analysis of biodegradable polymer blends of poly(sebacic anhydride) and poly(DL-lactic acid). Macromolecules 1996;29:2205–12.